EasyChair Preprint

№ 9652

# Synthesis and Morphological Studies of Cerium Oxide-Zinc Oxide as a Potential Heterostructured Material

Sharifah Zahratul Ashirah Syed Abdullah,
Wan Rafizah Wan Abdullah, Fazilah Ariffin and
Mohd Sabri Mohd Ghazali



February 3, 2023

# Synthesis and Morphological Studies of Cerium Oxide-Zinc Oxide as A Potential Heterostructured Material

**Sharifah Zahratul Ashirah Syed Abdullah**[1*], Wan Rafizah Wan Abdullah[1], Fazilah Ariffin[2], Mohd Sabri Mohd Ghazali[2]

[1]Faculty of Ocean Engineering Technology and Informatics, Universiti Malaysia Terengganu, 21030 Kuala Nerus, Terengganu, Malaysia

Email: p4967@pps.umt.edu.my**;** wanrafizah@umt.edu.my

[2]Faculty of Science and Marine Environment, Universiti Malaysia Terengganu, 21030 Kuala Nerus, Terengganu, Malaysia

Email: fazilah@umt.edu.my; mohdsabri@umt.edu.my

## Abstract

ZnO is an attractive material with a direct band gap energy of 3.3 eV and binding energy of 60 meV for basic research and industrial applications. However, there are several structural modifications being studied to increase the efficiency and functionality of ZnO for various potential applications. The construction of heterostructured system comprising multicomponent or multiphase is one of the most effective strategies to balance the harsh terms, owing to the tunable band structure and efficient electron-hole separation and transportation, where endow them with suitable properties. In the present work, the synthesis route and the morphological studies conducted on a $CeO_2$-ZnO heterostructured material were reported. The ZnO nanoparticles have been modified with nano-scaled $CeO_2$ *via* special nanofabrication technique that combined the citrate gelation technique and solid phase sintering at 1200˚C for 5 hours. The molar ration between $CeO_2$ and ZnO was varied in the range of 0.1:100, 1:100 and 10:100. The phase analyses of the synthesized $CeO_2$-ZnO heterostructure were carried out by using XRD meanwhile the microstructure and elemental analyses were carried by SEM and EDX.

Keywords: Zinc oxide, Cerium oxide, Heterostructure, Nanofabrication

## 1 Introduction

Development of heterostructured materials is quickly becoming a major area of material research topic. This new class of advanced materials do not only exhibit superior mechanical and physical properties but they also challenge our conventional understanding and intuition. The term 'heterostructured materials' refers to those that include heterogeneous constituent physical qualities that are greatly variable, or in the case of functional materials, excessively diverse physical properties. According to the definition mentioned before, there are several classification of heterostructured materials such as typical heterostructured materials [1] , heterogeneous lamella structures [2], gradient structures [3], [4], laminate structure [5], [6], dual/multi-phase structures [7], harmonic (core-shell) structures [8] and multimodal structures [9]. Materials are amenable to processing using existing industrial equipment, enabling low-cost industrial manufacturing. Despite the fact that heterostructures were first investigated in structural materials [1], current developments show that they offer significant potential for obtaining unique functional features by overcoming intractable choices between conflicting qualities as follows i) heterostructured permanent-magnet materials, ii) heterostructured thermoelectric materials, iii) heterostructured catalytic materials [10].

$CeO_2$-ZnO heterostructure is one of the materials that attract researchers for the recent years. This functional material is a combination of ZnO and $CeO_2$. As a pure component, the ZnO is a semiconducting material with a direct band gap energy of 3.3 eV and binding energy of 60 meV. ZnO is a fairly common chemical used as a pigment, a component of pharmaceuticals, and an activator of the vulcanization of rubber [11]. It is also considered for electrical and electronic applications because of their stability, high electron affinity, and excellent electron mobility [12]. On the other hands, $CeO_2$ or ceria is a significant rare earth metal oxide with multi-beneficial characteristics, such as its high band gap energy, high refractive index, high visible region optical transparency, and high oxygen storage capacity [13]. The broad band gap of $CeO_2$ (3.2-3.9 eV) causes light to be absorbed in the ultraviolet range. Ceria has been used extensively in a variety application, including oxygen ion conductor in solid oxide fuel cells, transparent to visible light and UV blockers and filters [14], [15], gas sensors [16], [17], catalyst and oxygen sensors (SOFCs). Coupling $CeO_2$ with ZnO as new form of functional heterostructured materials is one of the strategies to explore their useful synergistic properties for many potential applications.

In photocatalysis application, the use of $CeO_2$-ZnO heterostructured materials has been proposed as a solution for extending the light absorption capacity and efficiency of ZnO. Many interesting catalytic effects have been observed as two materials with different energy bandgaps in a single matrix are coupled to build a heterostructured materials [18]. These materials have enhanced quantum efficiency to achieve superior photocatalytic or antibacterial activity by exhibiting strong

absorption in the visible area [19], [20]. Due to the right energy levels, the presence of double heterojunction has a significant influence on the physical characteristics of multi-metal oxide-based nanocomposites, including an increase in carrier lifespan, an increase in charge separation, and an intensification of charge transformation [21], [22]. Due to the tunable band structure and effective electron hole separation and transportation, which endow them with the necessary properties, the construction of heterostructured photocatalyst systems containing multiple components or multiple phases is one of the most successful strategies to balance the harsh conditions. While in the area of hydrgen recovery technology, plasmonic scheme heterostructure such as Ag-ZnO-$CeO_2$ is thoughtfully constructed and employed for photocatalytic generation of $H_2$. Ag-ZnO-$CeO_2$ photocatalyst demonstrates greatly improved photocatalytic $H_2$ evolution under simulated sunshine irradiation, [23].

The effective development of $CeO_2$-ZnO heterostructured materials is made possible by proper selection of raw materials and systematic synthesis technique. The properties of the materials can be tunable by manipulating the synthesis paramaters and material compositions. Therefore, this study reported an alternative way to synthesis a $CeO_2$-ZnO heterostuctured material by using a nanofabrication approach that combining a ZnO nanoparticles together with Ce.

## 2 Methodology

### 2.1 Preparation of $CeO_2$-ZnO Heterostructured Photocatalyst via Nanofabrication Technique

ZnO nanoparticles (<50nm) was modified with a nano scaled $CeO_2$ *via* a special nanofabrication procedure that combines the citrate gelation technique and solid phase sintering. The gelation process started by mixing together ZnO nanoparticles, into the slurry of citric acid ($C_6H_8O_7$) and cerium (III) nitrate (Ce $(NO_3)_3$) gel solution for 5 hours at the temperature range of 70-80 ºC and agitation at 300 rpm. The precursor mixture was then dried in the oven at 120 ˚C for 19 hours. Next, the dried mixture underwent calcination for another 4 hours at 500˚C and it was followed with sintering for 5 hours at 1200 ˚C. The sintered powder was subsequently screened and reduced into micro-sized aggregates with the uniform particle size of 50-60 μm. The synthesis process was repeated to produce $CeO_2$-ZnO at varying molar ration between 0.1:100, 1:100, 10:100. Purely ZnO nanoparticles underwent similar heat treatment processes and compared as Control.

A series of examinations was carried to confirm the successful conversion of the raw materials into intended $CeO_2$-ZnO microparticles and the formation of heterojunctions between $CeO_2$ and ZnO. Phase analysis was carried out by using an X-Ray Diffractometer machine (Rigaku Miniflex II Model PW1710) with Cu $K\alpha$ radiation having a wavelength, λ of 1.54 Å. Meanwhile, the microstructure and

elemental analysis of the prepared samples was carried out by using Scanning Electron Microscopy (JEOL JFC-1600) and Field Emission Scanning Microscopy (SEM) (JEOL JSM 7600F) equipped with Energy dispersive X-ray spectroscopy (EDX).

## 3 Results and Discussion

### 3.1 Phase Analysis

Figure 1 shows the XRD patterns of ZnO nanoparticles, sintered ZnO, $CeO_2$, and $CeO_2$-ZnO heterostructured (0.1:100, 1:100, 10:100). The diffraction peaks in XRD patterns of ZnO nanoparticles (precursor) and sintered ZnO (Control) correspond to the reflection planes of the wurtzite hexagonal ZnO (PDF80-75). Meanwhile the peaks in the XRD patterns of as-synthesized $CeO_2$-ZnO samples show additional peaks corresponding to the reflection planes of the cubic fluorite-structured $CeO_2$ (PDF 81-792). The intensity of characteristic peaks of $CeO_2$ located at 2θ of 29 $^o$ and 33 $^o$ which correspond to the (111) and (200) planes can be seen increasing with higher ratio of $CeO_2$. This evidence indicates that the $CeO_2$-ZnO obtained at the end of the synthesis process was a dual-phase highly crystalline system and the $CeO_2$ have been successfully coupled to the ZnO.

### 3.2 Microstructure of $CeO_2$-ZnO Heterostructured Materials

Figure 2 shows the microstructures of $CeO_2$-ZnO under SEM and the comparison to their pure components. It visualized that the size of ZnO increases after calcination and sintering processes. A series annealing treatments is believed to cause the ZnO grains to grow from nano-scaled to micron-scaled. However, the incorporation of $CeO_2$ had caused pinning effects that suppressed the ZnO growth. For that reason, the ZnO grains in $CeO_2$-ZnO appeared to be relatively smaller than the purely sintered ZnO particularly for molar ration of 10:100. Close observation on the SEM images of $CeO_2$-ZnO material proved that the $CeO_2$ phase preferentially segregate as nodules on top of the ZnO grains. Each nodule is expected to contain clusters of nanoscaled $CeO_2$. As a result, the $CeO_2$ nodules can be seen decorating the ZnO surface. The size of the nodules enlarged while its distribution widened as the molar ration of the $CeO_2$ was increased from 0.1 to 10.

Figure 3 depicts the FESEM-EDX analysis performed on $CeO_2$-ZnO sample at 1.0:100 molar ration. This sample represents the synthesized heterostructured materials. EDX point mapping indicates the elemental distribution at three specific spots on the sample. The findings supported that the Ce element mostly found accumulating as bright nodules on top of the grains. This is consistent with the observation in SEM analysis. Segregation of phases after high temperature sintering is a common phenomenon. The $Ce^{3+}/Ce^{4+}$ ion with larger ionic size (0.097 - 0.114 nm)

than $Zn^{2+}$ (0.074 nm) will have higher tendency to segregate outside of ZnO crystal rather than diffusing into it. The higher the composition of $Ce^{3+}/Ce^{4+}$, the more obvious the phase segregation would be. Such structure is intentional in the making of heterostructured materials because every point of contact between $CeO_2$ and ZnO may contribute to formation of heterojunction. Therefore, higher $CeO_2$ ratio would contribute to creation of more heterojunctions.

The addition of $CeO_2$ into the ZnO through citrate gelation technique and sintering had tranformed the material into a dual or multi-phase structure. According to Zhu et al., (2021), dual or multiphase structure is a class of structural heterostructed materials. Other forms of heterostructured materials may include the lamella, gradient, laminate, core-shell and multi-modal structures. Diversity of these microstructures will determine their unique mechanical, physical, electrical and optical characteristics.

## 4 Conclusion

In conclusion, dual or multi-phase $CeO_2$-ZnO heterostructured were successfully obtained via nanofabrication technique reported in this paper. The heterojunctions formed due to significant phase segregation between $CeO_2$ and ZnO during sintering process. The ratio of $CeO_2$ to ZnO influenced the number of heterojunctions formation and the grain size of the ZnO. With further electrical, mechanical and physicochemical characterizations, the impact of the $CeO_2$-ZnO molar ration on these properties can be evaluated.

## Acknowledgements

The author would like to thank Universiti Malaysia Terengganu and Ministry of Higher Education for funding this project under the Talent and Publication Enhancement- Research Grant (TAPE-RG) Vot number: 55215.

## References


[1] X. Wu and Y. Zhu, “Heterogeneous materials: a new class of materials with unprecedented mechanical properties,” *Mater. Res. Lett.*, vol. 5, no. 8, pp. 527–532, 2017.

[2] X. Wu *et al.*, “Heterogeneous lamella structure unites ultrafine-grain strength with coarse-grain ductility,” *Proc. Natl. Acad. Sci. U. S. A.*, vol. 112, no. 47, pp. 14501–14505, 2015.

[3] X. Wu, P. Jiang, L. Chen, F. Yuan, and Y. T. Zhu, “Extraordinary strain hardening by gradient structure,” *Proc. Natl. Acad. Sci. U. S. A.*, vol. 111, no. 20, pp. 7197–7201, 2014.

[4] N. Makeswaran, C. Orozco, A. K. Battu, E. Deemer, and C. V. Ramana, “Structural, Optical and Mechanical Properties of Nanocrystalline Molybdenum Thin Films Deposited under Variable Substrate Temperature,” *Materials (Basel).*, vol. 15, no. 3, 2022.

[5] X. Ma *et al.*, “Mechanical properties of copper/bronze laminates: Role of interfaces,” *Acta Mater.*, vol. 116, pp. 43–52, 2016.

[6] I. Bonadies, “Chapter 8 - Nanoscale Materials in Water Purification,” in *Micro and Nano Technologies*, S. Thomas, D. Pasquini, S.-Y. Leu, and D. A. B. T.-N. M. in W. P. Gopakumar, Eds. Elsevier, 2019, pp. 231–246.

[7] M. Calcagnotto, Y. Adachi, D. Ponge, and D. Raabe, “Deformation and fracture mechanisms in fine- and ultrafine-grained ferrite/martensite dual-phase steels and the effect of aging,” *Acta Mater.*, vol. 59, no. 2, pp. 658–670, 2011.

[8] A. Shokry, A. Ahadi, P. Ståhle, and D. Orlov, “Improvement of structural efficiency in metals by the control of topological arrangements in ultrafine and coarse grains,” *Sci. Rep.*, vol. 11, no. 1, pp. 1–14, 2021.

[9] B. Q. Han, J. Y. Huang, Y. T. Zhu, and E. J. Lavernia, “Strain rate dependence of properties of cryomilled bimodal 5083 Al alloys,” *Acta Mater.*, vol. 54, no. 11, pp. 3015–3024, 2006.

[10] E. Ma and T. Zhu, “Towards strength–ductility synergy through the design of heterogeneous nanostructures in metals,” *Mater. Today*, vol. 20, no. 6, pp. 323–331, 2017.

[11] M. Bahrami and A. Nezamzadeh-Ejhieh, “Effect of the supported ZnO on clinoptilolite nano-particles in the photodecolorization of semi-real sample bromothymol blue aqueous solution,” *Mater. Sci. Semicond. Process.*, vol. 30, pp. 275–284, 2015.

[12] A. Wibowo *et al.*, “ZnO nanostructured materials for emerging solar cell applications,” *RSC Adv.*, vol. 10, no. 70, pp. 42838–42859, 2020.

[13] Z. Cui, D. Zhang, J. Hu, and C. Fang, “CdS/CeO2 heterostructures as visible-light photocatalysts for the reduction of nitro to amine organics,” *J. Alloys Compd.*, vol. 885, p. 160961, 2021.

[14] Y. He, B. Yang, and G. Cheng, “Controlled synthesis of CeO2 nanoparticles

from the coupling route of homogenous precipitation with microemulsion," *Mater. Lett.*, vol. 57, no. 13–14, pp. 1880–1884, 2003.

[15] G. Li *et al.*, "Enhanced visible-light-driven photocatalytic inactivation of Escherichia coli using g-C3N4/TiO2 hybrid photocatalyst synthesized using a hydrothermal-calcination approach," *Water Res.*, vol. 86, pp. 17–24, 2015.

[16] N. Izu, T. Itoh, M. Nishibori, I. Matsubara, and W. Shin, "Effects of noble metal addition on response of ceria thick film CO sensors," *Sensors Actuators, B Chem.*, vol. 171–172, pp. 350–353, 2012.

[17] B. Renganathan, D. Sastikumar, G. Gobi, N. R. Yogamalar, and A. C. Bose, "Gas sensing properties of a clad modified fiber optic sensor with Ce, Li and Al doped nanocrystalline zinc oxides," *Sensors Actuators, B Chem.*, vol. 156, no. 1, pp. 263–270, 2011.

[18] T. Munawar *et al.*, "Structural, optical, electrical, and morphological studies of rGO anchored direct dual-Z-scheme ZnO-Sm2O3–Y2O3 heterostructured nanocomposite: An efficient photocatalyst under sunlight," *Solid State Sci.*, vol. 106, no. May, p. 106307, 2020.

[19] F. T. Johra and W. G. Jung, "RGO-TiO2-ZnO composites: Synthesis, characterization, and application to photocatalysis," *Appl. Catal. A Gen.*, vol. 491, no. 1, pp. 52–57, 2015.

[20] M. Rani and U. Shanker, "Sun-light driven rapid photocatalytic degradation of methylene blue by poly(methyl methacrylate)/metal oxide nanocomposites," *Colloids Surfaces A Physicochem. Eng. Asp.*, vol. 559, no. September, pp. 136–147, 2018.

[21] H. Zhao, X. Ding, B. Zhang, Y. Li, and C. Wang, "Enhanced photocatalytic hydrogen evolution along with byproducts suppressing over Z-scheme CdxZn1−xS/Au/g-C3N4 photocatalysts under visible light," *Sci. Bull.*, vol. 62, no. 9, pp. 602–609, 2017.

[22] D. Zeng *et al.*, "Phase transformation and microwave hydrothermal guided a novel double Z-scheme ternary vanadate heterojunction with highly efficient photocatalytic performance," *Appl. Catal. B Environ.*, vol. 237, no. May, pp. 449–463, 2018.

[23] A. Hezam *et al.*, "Rational construction of plasmonic Z-scheme Ag-ZnO-CeO2 heterostructures for highly enhanced solar photocatalytic H2 evolution," *Appl. Surf. Sci.*, vol. 541, no. November 2020, p. 148457, 2021.

List of Figure Captions

| Figure | Caption |
|---|---|
| Figure 1 | XRD patterns of the syntesized $CeO_2$-ZnO heterostuctured materials in comparison to ZnO nanoparticles, sintered ZnO and $CeO_2$. |
| Figure 2 | SEM images of a) ZnO nanoparticles b) $CeO_2$ c) Sintered ZnO and as-synthesized $CeO_2$-ZnO at molar ration of d) 0.1:100 e) 1:100 f) 10:100 |
| Figure 3 | FESEM-EDX spectrum of as-synthesized $CeO_2$-ZnO at molar ration 1:100 |

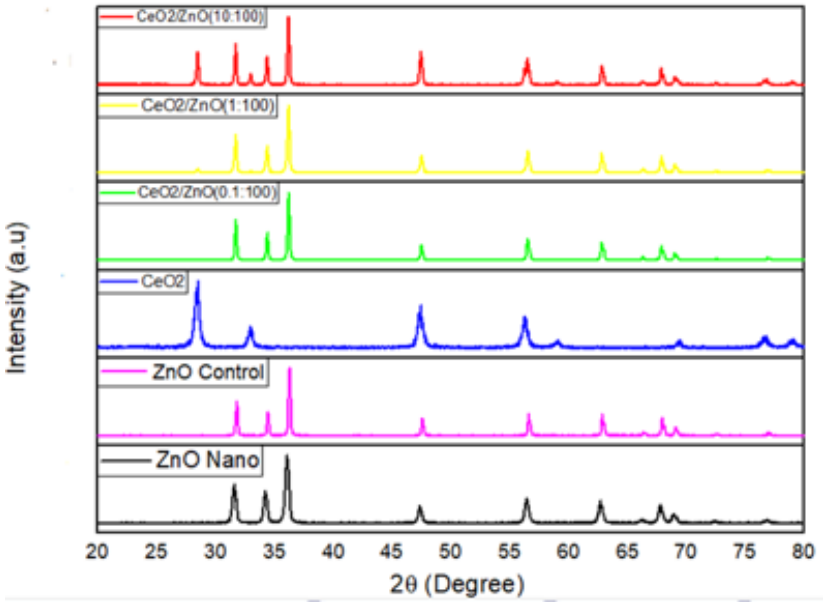


Figure 1: XRD patterns of the syntesized $CeO_2$-ZnO heterostuctured materials in comparison to ZnO nanoparticles, sintered ZnO and $CeO_2$.

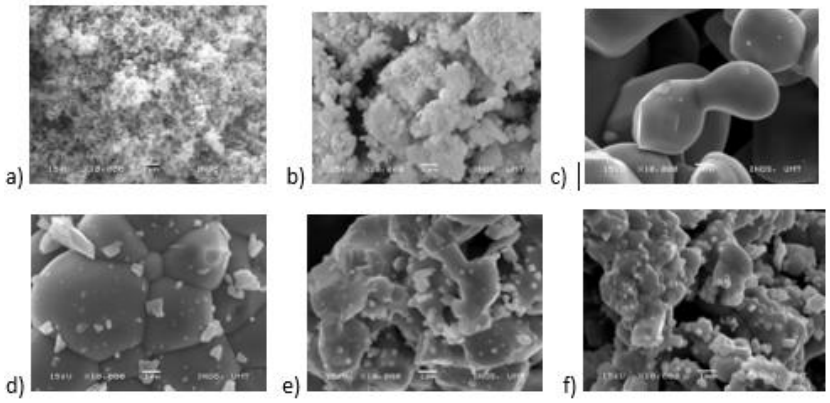


Figure 2: SEM images of a) ZnO nanoparticles b) $CeO_2$ c) Sintered ZnO and as-synthesized $CeO_2$-ZnO at molar ration of d) 0.1:100 e) 1:100 f) 10:100

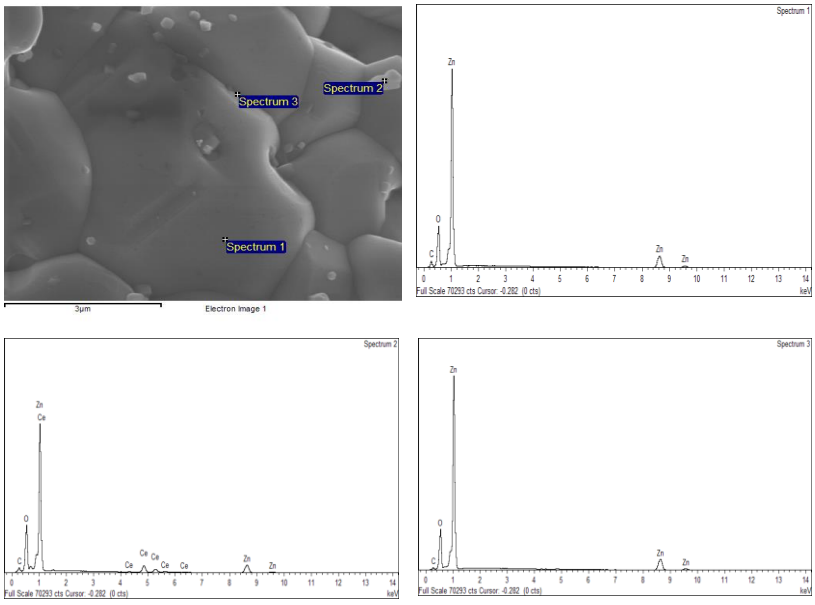


Figure 3. FESEM-EDX spectrum of as-synthesized $CeO_2$-ZnO at molar ration 1:100